frontiers | Frontiers in Marine Science

ORIGINAL RESEARCH
published: 06 June 2022
doi: 10.3389/fmars.2022.879388

Detection of Prokaryotes on the Astomatous Ciliated Protist *Kentrophoros flavus* (Ciliophora, Karyorelictea) Revealed A Consistently Associated *Muribaculaceae*-Like Bacterium

Luping Bi[1], *Xiaoxin Zhang*[1,2], *Songbao Zou*[3], *Daode Ji*[1]* and *Qianqian Zhang*[2,4]*

[1] School of Ocean, Yantai University, Yantai, China, [2] Key Laboratory of Coastal Environmental Processes and Ecological Remediation, Yantai Institute of Coastal Zone Research, Chinese Academy of Sciences, Yantai, China, [3] Key Laboratory of Fish Health and Nutrition of Zhejiang Province, Zhejiang Institute of Freshwater Fisheries, Huzhou, China, [4] Muping Coastal Environment Research Station, Yantai Institute of Coastal Zone Research, Chinese Academy of Sciences, Yantai, China

OPEN ACCESS

Edited by:
Alexey Potekhin,
Saint Petersburg State University, Russia

Reviewed by:
Valentina Serra,
University of Pisa, Italy
Marcus Vinicius Xavier Senra,
Universidade Federal do ABC, Brazil

***Correspondence:**
Daode Ji
daodeji@126.com
Qianqian Zhang
qqzhang@yic.ac.cn

Specialty section:
This article was submitted to Microbial Symbioses, a section of the journal Frontiers in Marine Science

Received: 19 February 2022
Accepted: 03 May 2022
Published: 06 June 2022

Citation:
Bi L, Zhang X, Zou S, Ji D and Zhang Q (2022) Detection of Prokaryotes on the Astomatous Ciliated Protist Kentrophoros flavus (Ciliophora, Karyorelictea) Revealed A Consistently Associated Muribaculaceae-Like Bacterium. Front. Mar. Sci. 9:879388. doi: 10.3389/fmars.2022.879388

The interactions between symbiotic bacterial consortia and their protist hosts in benthic environments have attracted increasing interest in recent years. In the present study, we investigated the diversity of potentially associated bacteria for an astomatous ciliate, *Kentrophoros flavus*, collected in the intertidal zone of Yantai, China. For the first time, the diversity of the associated bacteria in the species *K. flavus* was examined using 16S rRNA-based techniques (clone libraries and PacBio sequencing) and the fluorescence *in situ* hybridization (FISH) technique. The 16S rRNA-based sequencing revealed a higher diversity of associated bacteria in *K. flavus* than previously expected. In addition to a genus-typical thiotrophic symbiont, the "*Candidatus* Kentron" stain YE, we provide evidence showing the consistent existence of one *Muribaculaceae*-like bacterium that was secondarily abundant among the bacterial operational taxonomic units (OTUs). Fluorescence *in situ* hybridization (FISH) with three specific probes and double-label FISH experiments with "*Candidatus* Kentron" probes showed that the *Muribaculaceae*-like bacterium was abundant and merged with the "*Candidatus* Kentron" stain YE on the cell surface of the host. A phylogenetic analysis of the bacterial 16S rRNA gene showed that the bacterium was a distinct branch in *Muribaculaceae*, members of which are primarily reported from gut microbiome. The name "*Muribaculaceae*-like bacterium associated with *Kentrophoros flavus*" (MLAKF) is proposed for the new bacterium. The higher 16S rRNA diversity in *K. flavus* and the discovery of MLAKF on the cell surface both suggest a potential bacterial consortium that interacts with the host *K. flavus*.

Keywords: *Kentrophoros*, symbiosis, bacterial diversity, ciliate, *Muribaculaceae*

INTRODUCTION

Ciliates are widespread unicellular organisms in marine benthic environments (Choi et al., 2012; Cai et al., 2013) that include some extreme habitats (Wilbert and Song, 2005; Lei and Xu, 2008). One important mechanism that makes ciliates thrive in extreme environments (e.g., micro-aerobic/anoxic, sulfide-rich, high-nitrate) or grow on inaccessible diets in the sediment is harboring and interacting with symbiotic bacteria (Nowack and Melkonian, 2010). Recently, studies of the diversity of symbiotic bacteria associated with benthic ciliates have revealed novel bacterial species that possess specialized physical or biochemical traits (Embley et al., 1992; Rosati, 2002; Beinart et al., 2018; Lind et al., 2018; Graf et al., 2021). One well-known representative is the association of benthic ciliates with thiotrophic bacteria in which ectosymbionts account for approximately half the biomass of the symbiotic consortium in some species (Fenchel and Finlay, 1989). Ciliates associated with thiotrophic bacteria are known typically from two genera—the periphyton *Zoothamnium* and the benthic *Kentrophoros*—both of which are densely covered by ectosymbionts on the cell surface (Raikov, 1971; Fenchel and Finlay, 1989; Edgcomb et al., 2011; Bright et al., 2014; Seah et al., 2017). Evidence has shown that thiotrophic symbionts can absorb and oxidize sulfide in sulfur-rich environments (Fenchel and Finlay, 1989; Volland et al., 2018; Seah et al., 2019). The symbionts are phagocytized by the host as a food resource (Foissner, 1995; Dubilier et al., 2008; Bright et al., 2014) or directly release soluble organic molecules that are uptaken into the host cytoplasm (Volland et al., 2018). Mutually, the ciliate host may carry the ectosymbionts to a depth in sediments where the chemical gradients are not too steep and where the bacterial metabolisms are optimized (Fenchel and Finlay, 1989).

Some ciliates host more than one symbiotic (or associated) species that may form structural and functional consortia (Edgcomb et al., 2011; Park and Yu, 2018; Lanzoni et al., 2019; Muñoz-Gómez et al., 2021). Functional consortia have been recovered in a geleiid karyorelictean ciliate that harbored two sulfate reducers, a methanogen, and possibly a Bacteroidetes and a Type I methanotroph (Edgcomb et al., 2011). A purple-green ciliate, *Pseudoblepharisma tenue*, was found simultaneously harboring green algae and anoxygenic photosynthesizers (e.g., purple bacteria) (Muñoz-Gómez et al., 2021). Boscaro et al. (2019) found that up to six different symbionts could co-occur in the cytoplasm of a single *Euplotes* species. In ciliates associated with thiotrophic bacteria, much less attention has been paid to the diversity and composition of the ectosymbionts, although single thiotrophic bacterial species have been recognized in *Zoothamnium* ("*Candidatus* Thiobios zoothamnicoli", *Gammaproteobacteria*) and *Kentrophoros* ("*Candidatus* Kentron spp.", *Gammaproteobacteria*) (Bright et al., 2014; Seah et al., 2017; Seah et al., 2019).

Members of the genus *Kentrophoros* (Ciliophora and Karyorelictea) are microaerobic ciliates that are typically distributed in the chemocline between the oxidized and anaerobic sulfide–reducing layers of marine sediments (Fenchel, 1969). They are typically characterized by a lack of the adoral zone for prey, but they are covered with dense rod-shaped chemolithotrophic bacteria on the cell surface (Foissner, 1995; Gao et al., 2010; Xu et al., 2011). It has been shown that this ciliate relies directly on engulfing symbionts (or adhering algae/particles) along the entire cell body as a food resource (Fenchel and Finlay, 1989; Foissner, 1995). Morphological observation and chemical measurement estimated that one *Kentrophoros* cell carries approximately 4500 bacteria that account for approximately half the biomass of the symbiont-ciliate consortium (Fenchel and Finlay, 1989). Earlier ultrastructural observations (Fenchel and Finlay, 1989; Foissner, 1995) and recent metagenomic methods (Seah et al., 2017) have both revealed sulfur-oxidizing bacteria among the symbionts. Using the meta-genome technique and 16S rDNA amplification, Seah et al. (2017; 2019) recognized one genus from 13 *Kentrophoros* spp. and proposed the name "*Candidatus* Kentron" (hereafter, "*Ca.* Kentron"). Despite being known as the primary food source for *Kentrophoros*, a genomic study of "*Ca.* Kentron" revealed that the thiotrophic bacteria lack genes that encode canonical enzymes for autotrophic CO_2 fixation (Seah et al., 2019). This indicates that there must be extra energy and organic carbon sources for the "Kentron-*Kentrophoros*" system from the environment or microbial activities (Seah et al., 2019). Thus far, there have been no systematic studies investigating the bacterial diversity associated with the genus *Kentrophoros* (symbiotic and/or adhering). It is unclear if "*Ca.* Kentron" is the only genus among the ectosymbionts or whether there are other bacteria that interact with the "Kentron-*Kentrophoros*" system.

In recent decades, molecular approaches such as 16S rDNA cloning and sequencing and fluorescence *in situ* hybridization (FISH) have been increasingly used to detect and identify bacterial symbionts or associations with unicellular eukaryotes (Edgcomb et al., 2011; Gong et al., 2014; Seah et al., 2017; Plotnikov et al., 2019). Most recently, the newly developed PacBio platform was able to generate more than 5000 CCS 16S rDNA sequences from one sample (with >0.99 accuracy for 16S rDNA fragments). This allows for a much deeper sequencing depth than is the case with rDNA clone libraries. These approaches make it possible to discover the potentially associated prokaryotes on *Kentrophoros* outside of "*Ca.* Kentron".

In this study, we collected and described a *Kentrophoros* species, *K. flavus*, from the intertidal region near the eastern gate of Yantai University (hereafter, *K. flavus* YE). The bacterial diversity associated with *K. flavus* YE was examined using 16S rRNA-based approaches, including the clone library and PacBio sequencing. We detected a genus-typical thiotrophic symbiont and named it the "*Candidatus* Kentron" stain YE (hereafter, "*Ca.* Kentron" YE). In addition, an undescribed bacterium belonging to the molecular family *Muribaculaceae* was also consistently detected in the PacBio data. The name "*Muribaculaceae*-like bacterium associated with *Kentrophoros flavus*" (MLAKF) is proposed for the bacterium. Three specific probes were designed, and *in situ* FISH was performed to determine the location of MLAKF on the ciliate cells.

MATERIALS AND METHODS

Sample Collection and Morphological Observations

Kentrophoros flavus YE was collected on different dates from May 2020 to March 2022 from the intertidal zone near the eastern gate of Yantai University, China (37°28′50″N, 121°27′41″E). Samples were scraped at the chemocline in fine, well-sorted sands with a reduced, sulfide layer at an approximate 15 cm beneath the sediment surface. Wet sands were transported to the laboratory and examined under a stereo microscope (Guiguang GL-6345BI, China). Living cells were observed using a bright field and differential interference contrast microscopy at 100-1000× magnifications (Zeiss Axio Scope A1, Germany). Counts and measurements of the living cells were conducted at a magnification of 1000×.

DNA Extraction, PCR Amplification, Clone Libraries, and PacBio Sequencing

Approximately 10 cells were isolated from the raw cultures using a micropipette and washed three times with *in situ* water filtered by a millipore filter of 0.2 μm in pore diameter (Pall Laboratory, US) to remove the irrelevant bacteria in the environmental water. The ciliate cells were then starved for approximately 5 h in the sterilized water, allowing the hosts to digest the potential bacterial food in the cytoplasm. Each individual was transferred into 1.5 ml Eppendorf tubes with a small drop of water for DNA extraction. DNA was extracted using the REDExtract-N-Amp Tissue PCR Kit (Sigma, St. Louis, MO) according to Gong et al. (2016).

The host's 18S rRNA gene was amplified *via* polymerase chain reaction (PCR) with the primers 82F (5′-GAAACT GCGAATGGCTC-3′) and 1492R (5′-GGTTACCTTGTTAC GACTT-3′) according to Wang et al. (2019). The PCR reaction solution (25 μl) contained 2 μl of 10 μM primers, 1 μl of template, 12.5 μl of MegaFi™ Fidelity 2X PCR MasterMix with MegaFi™ Fidelity DNA Polymerase (ABM, Shanghai, China), and 9.5 μl of nuclease-free H_2O. The cycling parameters were as follows: pre-run of 3 min at 95°C, followed by 30 cycles of 30 s at 95°C, 30 s at 56°C, and 90 s at 72°C, with a final extension of 10 min at 72°C. The associating bacteria's 16S rRNA gene was amplified *via* PCR with the primers 27F (5′-AGAGTTTGATCMTGGCTCAG-3′) and 1525R (5′-AAGGAGGTGATCCAGCC-3′). The PCR reaction solution (25 μl) contained 2 μl of 10 μM primers, 1 μl of template, 0.5 μl of dNTP Mix (10 mM of each), 1.25 units of Vazyme Lamp® DNA Polymerase (Vazyme, Nanjing, China), 2.5 μl 10X of Vazyme Lamp® buffer with $MgCl_2$, and 18.75 μl of nuclease-free H_2O. The cycling parameters were as follows: pre-run of 5 min at 94°C, followed by 30 cycles of 90 s at 94°C, 90 s at 53°C, and 3 min at 72°C, with a final extension of 10 min at 72°C. The PCR products were purified using a TIANgel Midi Purification Kit (Tiangen Bio. Co., Shanghai, China) and then inserted into pCE2 TA/Blunt-Zero vectors (5 min TA/Blunt-Zero Cloning Kit, Vazyme, Nanjing, China). The recombinant vectors were then transformed into competent cells Trans1-T1 (TransGen Biotech Co., Ltd., Beijing, China). The recombinants were screened using the blue/white selection. The white colonies were randomly selected and screened using PCR with the primers M13-20 and M13-26. Positive clones with the target inserts were sent for Sanger sequencing (Sangon Biotech Co., Ltd., Shanghai, China). A total of 132 clones were sent, and 46 sequences were successfully obtained, with an average length of 1500 bp.

For the other two ciliate individuals, the PacBio Sequel II platform was selected to complete the collection of the 16S rRNA full-length amplicons. The 16S rRNA gene was amplified using the same primers and PCR cycling parameters as those applied in the clone library construction. The PCR amplicons derived from two individuals were purified separately using the DNA Clean & Concentrator™-5 Kit (Zymo Research, Beijing, China), and each library was constructed according to the size of the amplified fragments (approximately 1500 bp). Sequencing was performed on a PacBio sequel II platform (Frasergen Co., Ltd., Wuhan, China), using a Hifi mode for small-insert (1.6kb) libraries, which allowed the insert being corrected by circular consensus sequences (CCS) for 30-40 times (with CCS≥3) and ensured an accuracy higher than 99.9%. More than 5000 raw CCS were generated from each sample.

Sequence Analysis for the Clone Library and the PacBio Data

Data derived from the clone libraries were examined manually to remove vector sections and low-qualified sequences using Bioedit (Hall et al., 2011). Data generated from PacBio sequencing were pretreated and qualified using the Pacific Biosciences' SMRT Link v8.0 workflow (https://www.pacb.com/support/software-downloads). Subreads were generated using the lima program integrated in SMRT Link inferring the barcode information of each sample. The subreads were converted to raw CCS using the CCS program with a strict threshold (minPasses≥3, minPredictedAccuracy≥0.99). Cutadapt V3.2 (Martin, 2011) was used to identify and trim the adapters from the raw CCS with a maximum error rate of 0.1. Chimeras and raw CCS shorter than 1300 bp were also filtered by Cutadapt V3.2.

The qualified clone sequences and clean CCS were pretreated following the methods of Fu et al. (2020). Briefly, chimeras were further removed using the vsearch program integrated in QIIME v.1.8.0 (Caporaso et al., 2010), and the singletons were discarded using Mothur v.1.34.4 (Schloss et al., 2009). The resulting data were clustered according to operational taxonomic units (OTUs) at a sequence similarity of 97% using QIIME v.1.8.0 (Caporaso et al., 2010). The OTUs were blasted, aligned, and classified against the SILVA ribosomal RNA gene database (SILVA 128 database, accessed October 2021) (Quast et al., 2012). Analysis of the species composition and abundance was conducted to examine the major taxa of the associated bacteria using the Pacman package (Peng et al., 2021) appended in R (v3.6.2).

Phylogenetic Analysis for Ciliate and the Associated Bacteria

For the phylogenetic analyses of the 18S rRNA gene (ciliate host), 34 sequences from the ciliate class Karyorelictea and 11

sequences of the class Heterotrichea were downloaded from the GenBank database and were appended to the new 18S rRNA sequences. Members of class Heterotrichea were selected as outgroups. Two separate phylogenetic analyses of 16S rRNA were performed for the bacterial OTUs "*Ca.* Kentron" YE and MLAKF. For "*Ca.* Kentron" YE, the reference sequences were revised from the dataset of Seah et al. (2017). A total of 42 16S rRNA sequences from the class *Gammaproteobacteria* were appended to the new sequences, and the classes *Coxiellaceae* and *Ectothiorhodospiraceae* were used as outgroups (Seah et al., 2017). For the OTU MLAKF, 44 sequences from the classes *Muribaculaceae*, *Bacteroidaceae*, *Prevotellaceae*, and *Porphyromonadaceae* of the phylum Bacteroidetes were appended. The classes *Bacteroidaceae*, *Prevotellaceae*, and *Porphyromonadaceae* were selected as outgroups (Lagkouvardos et al., 2019).

The assembled 16S and 18S rRNA datasets were first aligned using SINA v.1.2.11 integrated in the SILVA Web server (https://www.arb-silva.de/aligner/) with default parameters (Pruesse et al., 2012). The resulting alignments were refined manually to excise poorly aligned sites in SeaView v4.0 (Galtier et al., 1996). For the dataset of *K. flavus* YE, "*Ca.* Kentron" YE, and MLAKF, the final matrix used for the tree analysis comprised 1524, 1580, and 1505 nucleotide positions, respectively. The maximum likelihood (ML) and MrBayes v.3.2.2 (BI) algorithms were used to perform the phylogenetic tree analyses. In all three datasets, the GTR + I + Γ model was selected as the best model for both algorithms by jModelTest 2.1.7 (Posada, 2008) using the Akaike Information Criterion (AIC). The ML trees of the rRNA genes were constructed with RAxML V. 8 (Stamatakis, 2014) with 100 random taxon additions to generate the starting trees. Bootstrap support was inferred from 1000 pseudo replicate datasets. The Bayesian inference (BI) approach was implemented by MrBayes v.3.2.2 (Ronquist and Huelsenbeck, 2003). Markov chain Monte Carlo (MCMC) simulations were run for 5,000,000 generations (default temperature parameter and sampling frequency 0.01) with two parallel runs and each run with four simultaneous chains. The mean standard deviation of the split frequencies based on the last 75% of generations was 0.004 (< 0.01) at the end of the analysis. The first 12,500 trees (corresponding to 25% of generations) were removed as burn-in. MEGA v.6 (Tamura et al., 2013) was used to visualize tree topologies and adjust the branches.

Fluorescence *In Situ* Hybridization (FISH)

Three 16S rRNA-targeted oligonucleotide probes targeting MLAKF were newly designed according to the method of Gong et al. (2014), and they were named C01-612, C01-824, and C01-1125. The specificities of the probes were confirmed using the Test Probe 3.0 tool against the SILVA NR 99 database (https://www.arb-silva.de/search/testprobe/). The non-sense probe NON338, complementary to C01-612/824/1125, was used as a negative control for the hybridization protocol. The specific probe chr4Ca for "*Ca.* Kentron" (Seah et al., 2017) was also employed in our FISH analysis to virtualize "*Ca.* Kentron" YE. The primary sequence and specificity of the four probes are shown in **Table 1**.

The whole-cell hybridization procedure followed the protocol of Omar et al. (2017). Starved ciliates were transferred on microscopic slides (Frontier FRC-05) and dried at room temperature after fixation using Bouin's solution (50%, final concentration). Prior to the FISH assay, the slides were washed three times in distilled water and then progressively dehydrated *via* ethanol gradients (30%, 50%, 80%, and 100%). The concentration of formamide for each probe was estimated in the mathFISH webserver (http://mathfish.cee.wisc.edu/formamide.html) (Yılmaz and Noguera, 2007). The highest concentration (30%) among the three was applied to maximally remove unspecific hybridization (Gong et al., 2014). There was 36 μl of the hybridization buffer (20 mM Tris–HCl at pH 8.0, 0.9 M NaCl, 0.01% SDS = sodium dodecyl sulfate, and 30% formamide) added to the slides together with 4 μl of the targeting fluorescent probes (5 ng/μl final concentration). "Cy3" fluorescence was applied to all MLAKF probes (C01-612/824/1125). For the double label experiment, the MLAKF and "*Ca.* Kentron" YE probes were labeled with "Cy3" and "AF488", respectively. Considering the disparity in the bacterial abundance, the two probes were mixed in various ratios (3.5 μl Cy3-C01-612/824:0.5 μl AF488-chrCa and 2 μl Cy3-C01-824: 2 μl AF488-chrCa) when applied in the experiment. The slides were incubated at 46°C for 3 h. After hybridization, the slides were dipped in a washing buffer (20 mM of Tris-HCl at pH 8.0, 450 mM of NaCl, 0.01% SDS) for 15 min at 48°C and then washed in chilled distilled water three times for 30 s. The specimens on the slides were covered with anti-fade mounting medium (Beyotime, China) and DAPI (50 ng/ml) for 5 min in darkness prior to observations under an epifluorescence microscope (Olympus BX61, Japan) using a SPOT RT3 digital camera (SPOT Imaging Solutions, Sterling Heights, US) and mercury lamp accessories (Olympus U-RFL-T, Japan). Photomicrographs were colored using Image-pro plus 5.1.

RESULTS

Morphological Description of the Host

The size of the host ciliate was 200-460 × 16-36 μm *in vivo*, with a length:width ratio of 8-12:1 when fully extended (n=20;

TABLE 1 | Oligonucleotide probes used in FISH for the detection of the MLAKF bacteria and "*Candidatus* Kentron".

Probe	Sequence (5′ - 3′)	Specificity	Data source
C01-612	TTCGAGCCGTTGAAACTG	*Bacteroidetes*, *Muribaculaceae*	Present study
C01-824	AGAATGATCCCTGAGTGA	*Bacteroidetes*, *Muribaculaceae*	Present study
C01-1125	GTTGCTAACAGGTCAGGC	*Bacteroidetes*, *Muribaculaceae*	Present study
chr4Ca	CCGAGGATGTCAAAAGCAGG	*Gamma*, *Ca.* Kentron	Seah et al., 2017

Gamma indicates the bacterial class Gammaproteobacteria.

SD=71.5 and 7.8 for the length and width, respectively). The cells were highly flattened and had long ribbon shapes (**Figure 1A**). The body was curved (**Figure 1A**). The cells crawled along the bottom of the petri dish and attached to the substrate when stimulated. The ciliate had no cytostome. Nearly the entire dorsal surface of the cell was covered by rod-shaped bacteria that attached to the host erectly with one end (**Figures 1B–E**). Refractile globules (approximately 1 μm in diameter) were found within nearly all the rod-shaped bacteria (**Figures 1C, D**). The ventral side of the ciliates showed no symbiotic bacteria (**Figure 1E**).

Phylogenetic Analyses of the Host

The 18S rRNA gene sequence of *Kentrophoros flavus* YE was deposited in the GenBank database with the accession number OM421748. The acquired 18S rRNA gene fragment was 1566 bp long and had a GC content of 48.98%. The BLAST search on NCBI showed that this 18S rRNA gene fragment had the highest identity (99.68%) with that of the *K. flavus* isolate QD (the accession number FJ467505) (Gao et al., 2010). The ML and BI trees based on the 18S rRNA gene showed identical topologies (**Figure 2**) in which the new sequence of *K. flavus* YE clustered with two species, the *K. flavus* QD and one isolate of *K. gracilis*, with high support from the ML (97%) and BI (1.00).

Diversity of Bacteria Associated With *Kentrophoros flavus* YE, Revealed by Clone Library and PacBio Sequencing

A total of 46 clean 16S rRNA gene sequences were obtained from the clone library technique and were assigned to 17 OTUs (**Figure 3**). Proteobacteria accounted for a sizable proportion of the assemblages (80.43%, 37 sequences). The most abundant OTU was affiliated with the genus "*Candidatus* Kentron" (41.30%, 19 sequences). The other OTUs comprised only a few sequences that were closely related to the genera *Thalassolituus* (10.87%, 5 sequences), *Neisseria* (8.7%, 4 sequences), *Escherichia* (4.35%, 2 sequences), *Sphingobium* (4.35%, 2 sequences), *Streptococcus* (4.35%, 2 sequences), and "*Candidatus* Nitrososphaera" (4.35%, 2 sequences).

A total of 6154 and 4729 clean CCS reads were generated from the PacBio sequencing data for the two ciliate individuals, the total of which was clustered to 121 OTUs (**Figure 4**). Based on the total reads, the phylum Proteobacteria accounted for a considerable proportion of the assemblages (72.12%), followed by Bacteroidetes (10.63%) and Firmicutes (9.78%). The top three

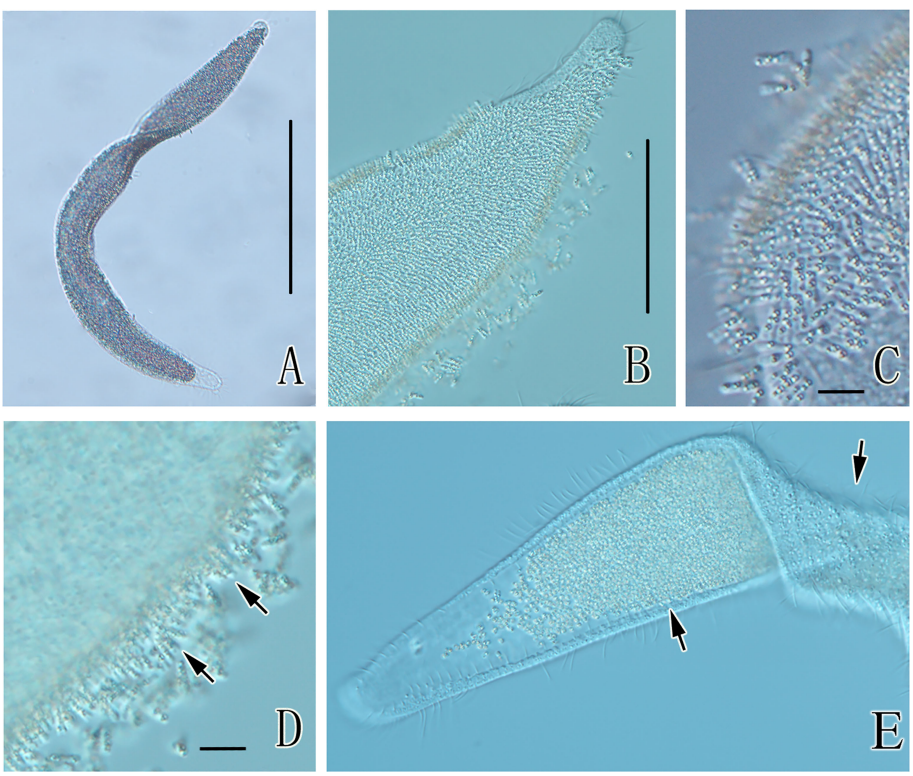

FIGURE 1 | Photomicrographs of *Kentrophoros flavus* YE from life. **(A)** Typical individual showing fold-over shape while gliding on the substrate; **(B)** showing the dense rod-shaped bacteria on the cell surface; **(C)** showing refractile globules within the rod-shaped bacteria; **(D)** details of the body margin showing rod-shaped bacteria (arrows); and **(E)** folded individual shows symbiotic bacteria on only one side (arrows). Scale bars = 100 μm **(A)**; 30 μm **(B, E)**; 5 μm **(C, D)**.

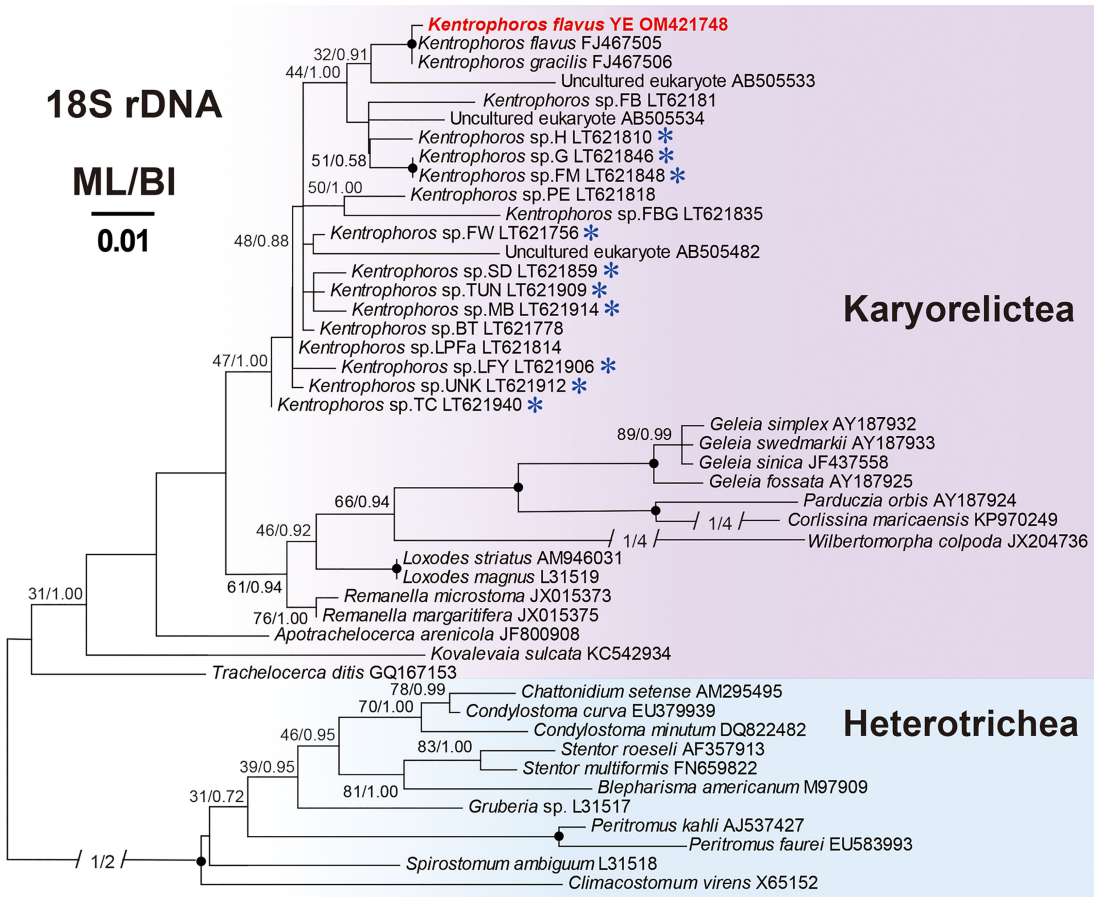

FIGURE 2 | Maximum likelihood (ML) tree based on the 18S rRNA genes showing the positions of *Kentrophoros flavus* YE (in red) with a GTR + I + Γ model. The numbers on the nodes represent the bootstrap values of the ML and the posterior probability of the Bayesian inference (BI). The black dot on the node represents the bootstrap value >95%. The species marked with blue asterisks have been reported with thiotrophic ectosymbionts. GenBank accession numbers are given following the species names. All branches are drawn to scale.

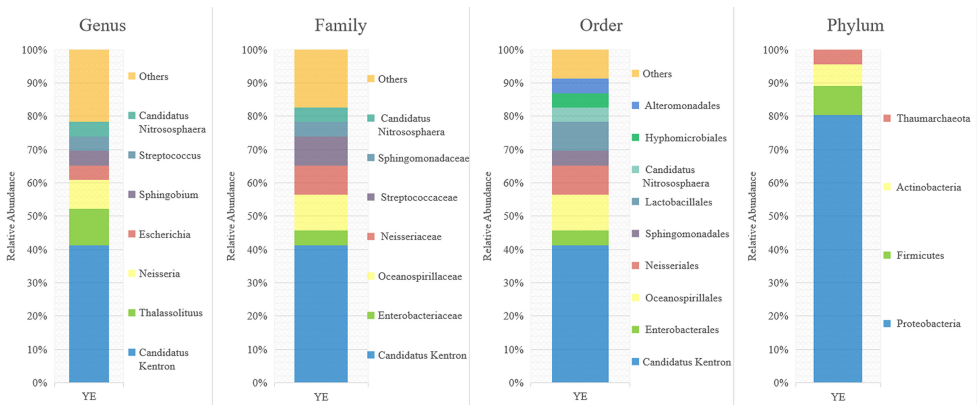

FIGURE 3 | Relative abundances of the bacterial major taxa in *Kentrophoros flavus* YE are suggested by the clone library data. Members of the genus, "*Candidatus* Kentron", are shown as the most frequently occurring bacteria.

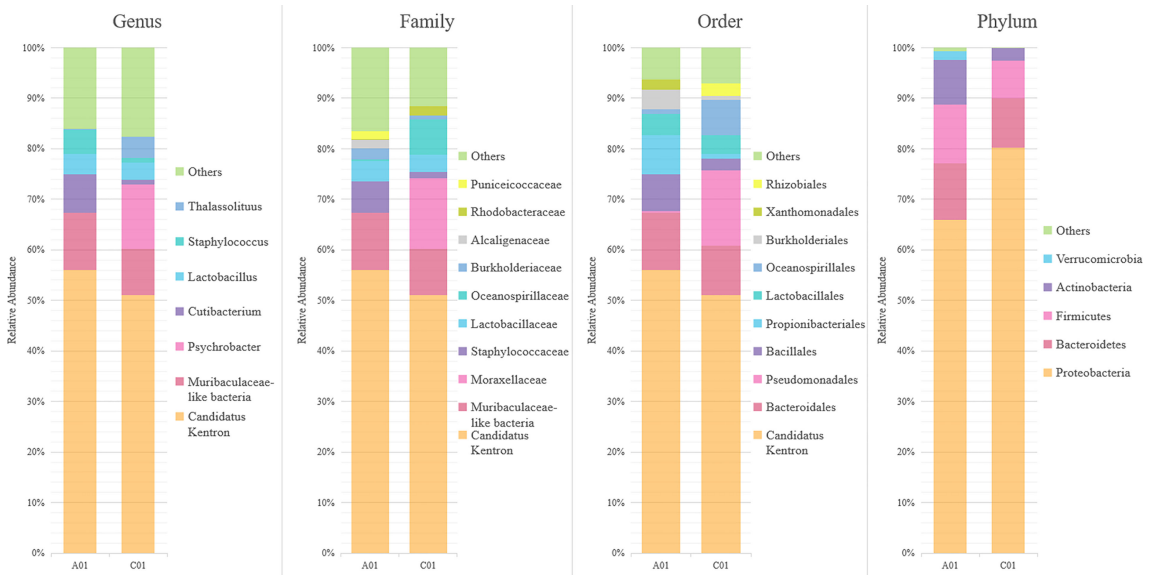

FIGURE 4 | Relative abundances of the bacterial major taxa in *Kentrophoros flavus* YE, inferred by the PacBio data. Note that the genera, "*Candidatus* Kentron" and *Muribaculaceae*-like bacteria, are shown as the most frequently occurring taxa. A01 and C01 represent different individuals of *Kentrophoros flavus* YE.

abundant bacterial orders were "*Ca.* Kentron" (53.89%), *Bacteroidales* (10.63%), and *Pseudomonas* (6.63%). The measurable OTUs (>2% relative abundance) were affiliated with 7 genera: "*Ca.* Kentron" (53.89%), *Muribaculaceae*-like bacteria (the formerly S24–7 group of *Bacteroidales*) (10.34%), *Psychrobacter* (5.53%), *Cutibacterium* (4.73%), *Lactobacillus* (3.74%), *Staphylococcus* (3.07%), and *Thalassolituus* (2.01%). Of the different ciliate individuals, the diversity of the most least abundant OTUs (<10%) varied obviously, for example, *Psychrobacter* (5.53% vs. 0.01%), *Cutibacterium* (4.32% vs. 0.41%), *Lactobacillus* (2.26% vs. 1.48%), *Staphylococcus* (2.69% vs. 0.38%), and *Thalassolituus* (1.86% vs. 0.15%). Nevertheless, the OTUs affiliated with "*Ca.* Kentron" and *Muribaculaceae*-like bacteria consistently occurred with the highest proportions in both individuals (**Figure 4**). Sequence of the former was nearly identical to the OTU affiliated with "*Ca.* Kentron" revealed in the Clone Library (differed by two bases). Accordingly, we named the two consistently occurring OTUs "*Ca.* Kentron" YE and "*Muribaculaceae*-like bacteria associated with *K. flavus*" (MLAKF). For the measurable OTUs in the PacBio data, the sequence length, GC content of the representative 16S rRNA, and the closely related sequences in the NCBI database gene fragments are provided in **Table 2**.

The 16S rRNA gene sequences of "*Ca.* Kentron" YE (derived from the Clone Library and the PacBio platform) and MLAKF were deposited in the GenBank database with accession numbers

TABLE 2 | Details of 16S rRNA gene fragments of "*Ca.* Kentron" YE and the measurable bacterial OTUs revealed by PacBio sequencing.

OTU name	OTU abundance	Sequence length	GC content	Closely related sequences (Genbank accession number) and identity	Closely related known species (Genbank accession number) and identity
Ca. Kentron YE OTU clone library	41.30%	1541	56.85%	*Ca.* Kentron H (LT622015) 95.43%	*Ca.* Kentron H (LT622015) 95.43%
Ca. Kentron YE OTU PacBio	53.89%	1510	56.62%	*Ca.* Kentron H (LT622015) 95.26%	*Ca.* Kentron H (LT622015) 95.26%
MLAKF	10.34%	1480	56.69%	Uncultured bacterium from environmental samples (EF406613) 98.58%	*Duncaniella* sp. C9 (MK521457) 96.83%
OTU-*Psychrobacter*	5.53%	1500	52.40%	Uncultured bacterium from environmental samples (KC502874) 99.87%	*Psychrobacter alimentarius* (JX514419) 99.86%
OTU-*Cutibacterium*	4.73%	1486	57.13%	Uncultured bacterium from environmental samples (MK372587) 99.93%	*Cutibacterium acnes* (KF933802) 99.53%
OTU-*Lactobacillus*	3.74%	1529	53.83%	Uncultured bacterium from environmental samples (FJ880299) 99.61%	*Limosilactobacillus reuteri* (MN537548) 99.54%
OTU-*Staphylococcus*	3.07%	1512	51.32%	*Staphylococcus hominis* (MH665980) 99.73%	*Staphylococcus hominis* (MH665980) 99.73%
OTU-*Thalassolituus*	2.01%	1500	53.46%	Uncultured bacterium (FJ403082) 98.8%	*Thalassolituus oleivorans* (KF170318) 97.78%

OM501125, OM501126, and OM468468. The read sequences derived from the PacBio sequencing were also deposited in GenBank, with the bioproject number PRJNA801354.

Phylogenetic Analyses of "*Ca.* Kentron" YE and the OTU MLAKF

Phylogenetic analyses based on the 16S rRNA genes were performed to assess the accurate affiliations of the OTU "*Ca.* Kentron" YE (**Figure 5**) and the OTU MLAKF (**Figure 6**). In the phylogenetic trees, "*Ca.* Kentron" YE fell into the clade of the genus "*Ca.* Kentron", belonging to the class *Gammaproteobacteria* (**Figure 5**). The BLAST search on the NCBI showed that this 16S rRNA gene fragment had the highest identity (95.43%) with that of "*Ca.* Kentron" H (accession number LT622015) (Seah et al., 2017). The OTU MLAKF fell into the family *Muribaculaceae* in phylum Bacteroidetes (100% ML/1.00 BI) (**Figure 6**). Within *Muribaculaceae*, MLAKF appeared to be a distinct taxon, as a sister branch to a clade comprising *Duncaniella* species and several uncultured bacteria (98% ML/1.00 BI) (**Figure 6**).

Fluorescence *In Situ* Hybridization (FISH)

The newly designed probes C01-824 and C01-612 for OTU MLAKF have been shown *in silico* to be highly *Muribaculaceae* specific in the SILVA NR 99 database (accessed March 2022). C01-824 completely matched the family *Muribaculaceae* (126/126). C01-612 primarily matched the family *Muribaculaceae* (151/154), except for one sequence of the family *Rikenellaceae* (Bacteroidetes) and two sequences of *Firmicutes* (*Bacteria*). The third probe, C01-1125, was more MLAKF-specific but matched a smaller range of *Muribaculaceae* (62/72). It also matched 10 sequences of the family *Prolixibacteraceae* (Bacteroidetes) and one sequence of *Thiomicrospiraceae* (*Gammaproteobacteria*). All matched non-*Muribaculaceae* families above were not detected in our clone library (**Figure 3**) and PacBio data (**Figure 4**), implying their absence in the samples. Compared to the 16S rDNA of "*Ca.* Kentron" YE, the three probes C01-612, C01-824, and C01-1125 were mismatched by 6, 7, and 7 sites, respectively, excluding the possibility of nonspecific binding to "*Ca.* Kentron" YE.

The three probes were applied separately to a total of 10 cells of *K. flavus* (4 cells with C01-612, 3 with C01-824, and 3 with C01-1125). Strong positive signals were observed on all specimens, with rod-shaped structures distinguishable on several slides (**Figures 7C, G, K**; **Figures 8C, H, M**). The overlays of the DAPI and probe's signals showed that the MLAKF bacteria were primarily located on the surface of the ciliate cells (**Figures 7D, H, L**). To distinguish MLAKF and "*Ca.* Kentron" YE, double-label experiments were conducted on the same ciliate with specific probes labeled with different fluorophores (**Figure 8**). For two sets of probe combinations, namely C01-612 + chr4Ca and C01-824 + chr4Ca, the red fluorescence (Cy3) of MLAKF (**Figures 8C, H, M**), and the green ones (AF488) of "*Ca.* Kentron" YE (**Figures 8D, I, N**) were simultaneously observed, both appearing on the host's surface. Negative control was conducted by using the non-sense probe NON338 (**Supplementary Figure S1**) in the FISH protocol, in which neither Cy3/AF488 fluorescence nor autofluorescence could be observed. Overlays of the signals on the same cell showed that the MLAKF and "*Ca.* Kentron" YE were mixed but were distinguishable from each other, with the former appearing more peripheral on the ciliate's cell surface (**Figures 8E, J, O**).

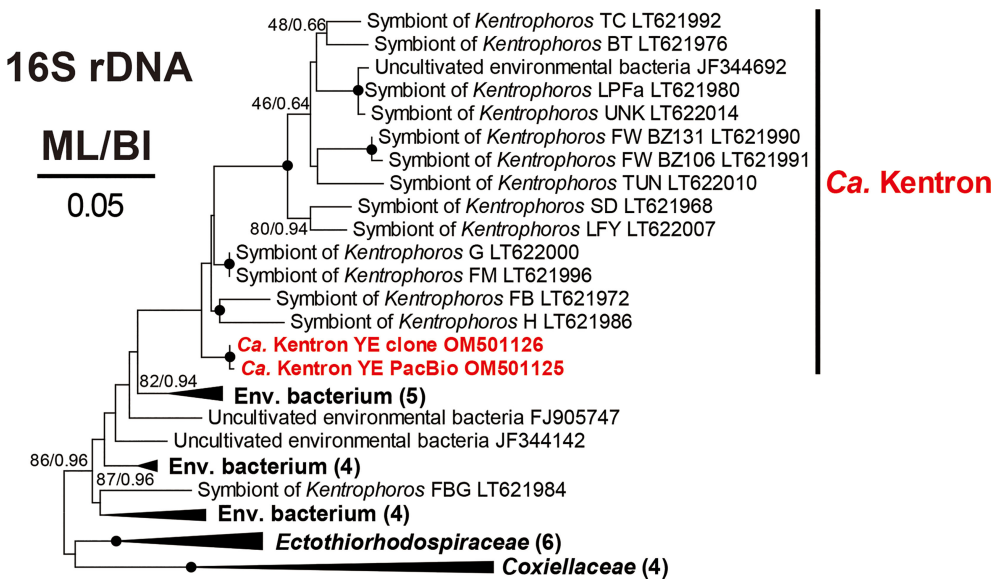

FIGURE 5 | Maximum likelihood (ML) tree based on the 16S rRNA genes showing the positions of "*Candidatus* Kentron" YE (in red) with a GTR + I + Γ model. The numbers on the nodes represent the bootstrap values of ML and the posterior probability of the Bayesian inference (BI). The black dot on the node represents the bootstrap value > 95%. Genbank accession numbers are given following the species names. All branches are drawn to scale.

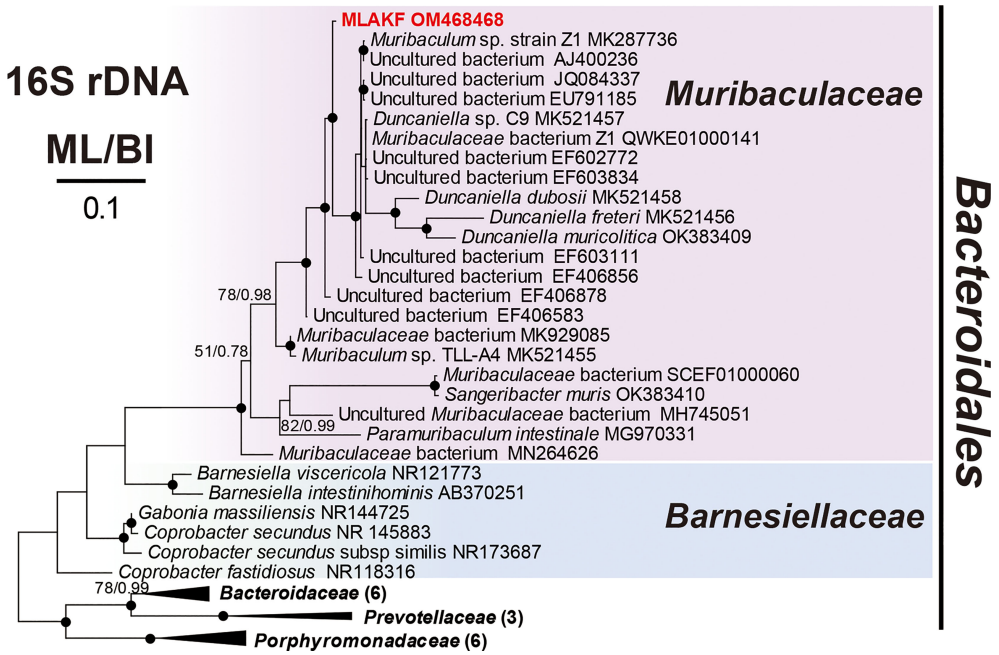

FIGURE 6 | Maximum likelihood (ML) tree based on the 16S rRNA genes showing the positions of MLAKF (in red) with a GTR + I + Γ model. The numbers on the nodes represent the bootstrap values of the ML and the posterior probability of the Bayesian inference (BI). The black dot on the node represents the bootstrap value > 95%. Genbank accession numbers are given following the species names. All branches are drawn to scale.

DISCUSSION

Comparison of the *K. flavus* YE and "*Ca*. Kentron" YE with Similar Species

The newly obtained 18S rRNA gene sequence for *Kentrophoros flavus* YE was closely clustered with *Kentrophoros gracilis* and *Kentrophoros flavus* (97% ML and 1.00 BI in both, **Figure 2**). In a comparison of the primary sequences, *K. flavus* YE differed from *K. flavus* and *K. gracilis* by 4 and 5 sites, respectively. *In vivo*, the Yantai populations matched the *K. flavus* population isolate in Qingdao (Xu et al., 2011) in terms of body shape and general appearance. In addition, the living cell characteristics of *K. flavus* YE were different from the original description of *K. gracilis* (Xu et al., 2011) in cell size (200–460 × 16–36 μm vs. 250–600 × 30–60 μm) and shape (*K. gracilis* was more elongated). The cells of *K. flavus* YE we observed were ciliated on the ventral side and contained ectosymbionts on the dorsal side (**Figure 1E**) corresponding to the "open" type among the four different body involution types recognized by Seah et al. (2017) for the genus *Kentrophoros*.

The OTU "*Ca.* Kentron" YE always displayed the highest proportion (41.3% in the clone library data and 53.89% in the PacBio data) among the *K. flavus*-associating bacteria (**Figures 3**, **4**). This aligns with the previous study that used the meta-genomic technique to detect the genus "*Ca.* Kentron" in 13 *Kentrophoros* morphospecies (Seah et al., 2017). Compared with the most similar relative, "*Ca*. Kentron" H (**Table 2**), "*Ca*. Kentron" YE was different by 70 bases in the primary 16S rRNA sequence, indicating that "*Ca.* Kentron" YE may represent a new ectosymbiotic species of the genus "*Ca.* Kentron".

Potential Roles of The Newly Detected MLAKF

As seen from the PacBio results (**Figure 4**), the OTU MLAKF accounted for the second-largest number (10.34%, approximately 1125 reads) among the associated bacteria in two *K. flavus* individuals. On 10 host cells that were sampled on different dates, the FISH results with three specific probes all produced positive signals of MLAKF on the surface of *K. flavus* (**Figures 7C, G, K**; **Figures 8C, H, M**), suggesting that their presence on the ciliate was relatively stable.

The 16S rRNA gene sequence of MLAKF was 21 bases different from an uncultured bacterium with 98.58% identity (**Table 2**), and 47 bases were different from the most similar species *Duncaniella* sp. C9 with 96.83% identity (accession number: MK521457). Combined with its distinct position in the phylogenetic trees (**Figure 6**), this suggests that MLAKF should represent a new bacterial species in the family *Muribaculaceae*. The family *Muribaculaceae* comprises mainly molecular taxa, which are known as prevalent and abundant bacterial components in the mammal gut microbiome (Lagkouvardos et al., 2019). Members of *Muribaculaceae* have been widely detected in the intestines of mice, humans, ruminants, and homeothermic animals (Van Valkenburgh, 1991; Salzman et al., 2002; Lagkouvardos et al., 2016; Lagkouvardos et al., 2019; Miyake et al., 2020), with only a few

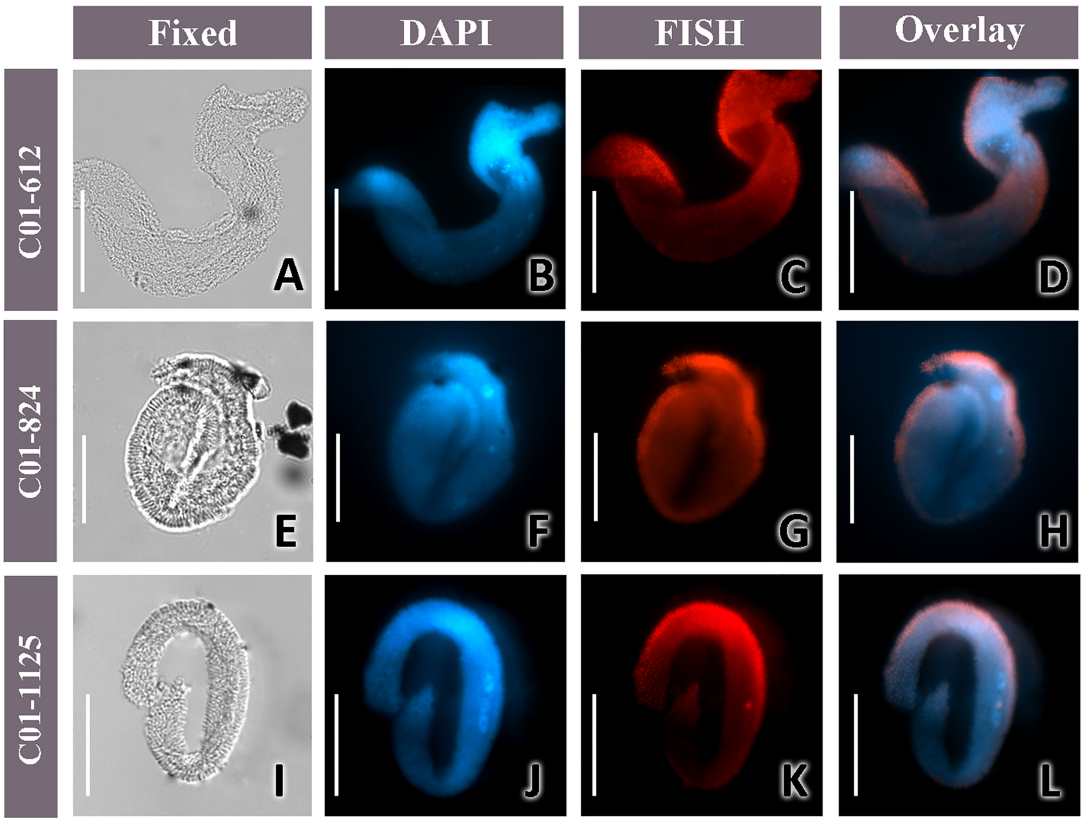

FIGURE 7 | Micrographs of *K. flavus* with MLAKF. **(A, E, I)** Microphotographs of the fixed cells in the bright field; **(B, F, J)** DAPI staining; **(C, G, K**), and fluorescence *in situ* hybridization (FISH) using Cy3-C01-612 **(C)**, Cy3-C01-824 **(G)**, and Cy3-C01-1125 probes **(K)**; **(D, H, L)** overlay of the DAPI and FISH. Scale bars = 50 μm **(A–L)**. The result for C01-824 was derived from a double-label experiment with a probe solution of 3.5 μl of Cy3-C01-824 plus 0.5 μl of AF488-chrCa, while others were generated from a single-probe (4-μl probe solution) hybridization.

species abundant in the natural environment, including manure, wastewater treatment plants, and coral reefs (Lagkouvardos et al., 2019). Our study adds to this list but with another scenario. Muribaculacid bacteria are abundant on the surface of the ciliated protist *K. flavus* and merge with thiotrophic ectosymbionts. This is the first time a muribaculacid bacterium has been found to be consistently associated with unicellular eukaryotic organisms.

It is worth noting that MLAKF was consistently present in large numbers on the cell surface of the host (**Figure 7**), emerging with or on an outlayer of the ectosymbiotic "*Ca.* Kentron" YE (**Figure 8**). The two symbionts and the ciliate host may have formed a three-partner consortium. First, MLAKF may offer extra organic carbon for the host-symbiont system. Genomic studies of "*Ca.* Kentron" have revealed that "*Ca.* Kentron" lacks genes encoding canonical enzymes for autotrophic CO_2 fixation, despite being a food source for *Kentrophoros* (Seah et al., 2019). It has been suggested that "*Ca.* Kentron" relies more on the uptake of exogenous organic substrates, heterotrophic carboxylation, and the recycling of host waste for growth (Seah et al., 2019). Extra energy and organic carbon sources should be required for the "Kentron-*Kentrophoros*" symbiote, and these should come from the environment or microbial activities (Seah et al., 2019). Coincidently, bacteria of *Muribaculaceae* have been predicted to play important roles in degrading dietary carbohydrates in the animal gut (Lagkouvardos et al., 2019). Genomic studies on a wide range of muribaculacid members have highlighted their prevalent versatility in degrading complex carbohydrates, benzoate resistance, and nitrogen utilization (>90% prevalence) (Ormerod et al., 2016; Lagkouvardos et al., 2019). Therefore, it is possible that MLAKF on the ciliate cells may play similar roles, degrading a wide range of substrate in the sediment (this might also include host waste) for growth, whereby the bio-product may provide accessible organic carbon for "*Ca.* Kentron". Simultaneously, MLAKF themselves may offer an extra food source for the ciliate to support the overall growth of the host-symbiont system.

Second, it is known that *Kentrophoros* likely shuttles between oxic and anoxic zones in marine sediment with the ectosymbionts (Fenchel and Finlay, 1989; Seah et al., 2019). Under anoxic conditions, thiotrophic bacteria would not completely oxidize sulfide to sulfate, leading to less efficient energy generation (Seah et al., 2019). MLAKF may contribute as a compensated food source under anoxic conditions. Members of *Muribaculaceae* have been revealed to be well equipped with anti-oxygen strategies to support potential microaerobic growth (Ormerod et al., 2016).

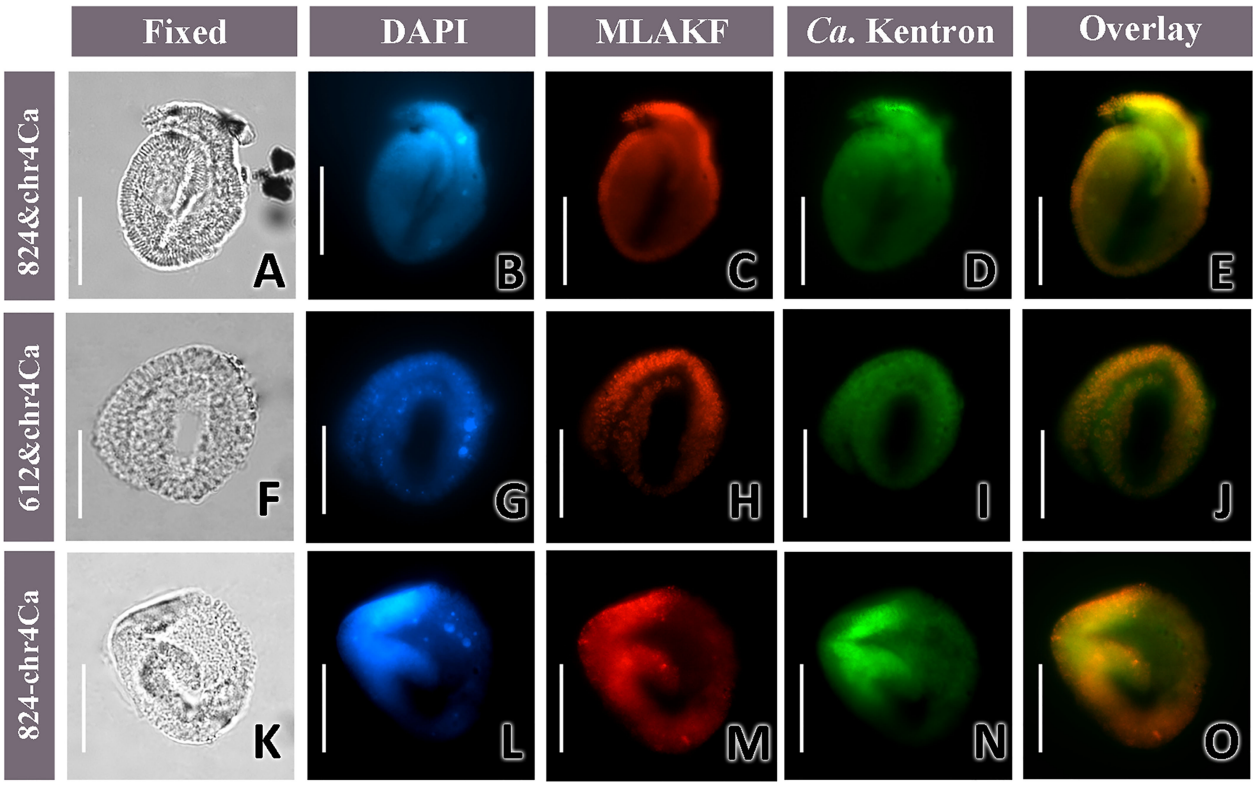

FIGURE 8 | Double-label experiments on the same cell with both the Cy3-C01-612/824 and AF488-chr4Ca probes; **(A, F, K)** microphotographs of the fixed cells in the bright field; **(B, G, L)** DAPI staining; **(C, H, M)** species-specific probes Cy3-C01-824 **(C, M)** and Cy3-C01-612 **(H)**; **(D, I, N)** species-specific probe AF488-chr4Ca; and **(E, J, O)** overlays of Cy3 and AF488 images. Scale bars = 50 μm **(A–O)**. For the cells in images **A** and **F**, the probe solutions of 3.5 μl of Cy3-C01-824/612 plus 0.5 μl of AF488-chrCa were applied, while for the one in **K**, 2 μl of Cy3-C01-824 plus 2 μl of AF488-chrCa were applied.

Nevertheless, the nature of the relationship between the MLAKF bacterium, "*Ca.* Kentron" YE, and *K. flavus* remains to be resolved, and single-cell genome sequencing can be a powerful tool for revealing the interactions between ciliated protists and their bacterial symbionts (Martinez-Garcia et al., 2012).

Higher Bacterial Diversity Potentially Associated With *K. flavus*

Aside from the thiotrophic bacteria "*Ca.* Kentron" YE, we detected a high diversity of associated bacteria using 16S rDNA-based approaches (**Figures 3** and **4**; **Table 2**). This result accords with a previous morphological study of the species *K. latum* that recorded ectosymbiotic spirochaetes and intracellular prokaryotic symbionts (Raikov, 1971). The existence of particles adhering to thiotrophic bacteria has also been observed (Fenchel, 1969; Fenchel and Finlay, 1989) (e.g., diatoms and other ingested particles within *Kentrophoros*), which may be another explanation for the high bacterial diversity being detected. Except for the overwhelming OTU "*Ca.* Kentron" YE, the revealed diversity of the associating bacteria in *K. flavus* was variable between the clone library and PacBio sequencing (**Figures 3**, **4**). This might be attributable to the significant difference in sequencing depths between the two techniques (46 clones vs. 10,883 CCS).

In addition to the consistently associated MLAKF bacterium, the comprehensive sequencing by the PacBio platform also detected OTUs related to members in the genera *Psychrobacter*, *Cutibacterium*, *Lactobacillus*, *Staphylococcus*, and *Thalassolituus*, all with measurable abundance (2–5.53%) (**Figure 4**; **Table 2**). Most of these 16S rDNA fragments are most similar to the known species in GenBank (**Table 2**), indicating that these might represent common taxa. Among these, members of *Cutibacterium* and *Psychrobacter* are obligate symbionts in human skin and the anogenital gland of captive pandas (Scholz and Kilian, 2016; Zhou et al., 2021), suggesting their symbiotic potential. However, the sequences might also derive from particles adhering to "*Ca.* Kentron", as assumed by previous morphological studies (Fenchel, 1969). Because of the variable result among the different individuals and a lack of FISH analysis, we must refrain from predicting the stable existence or roles of these OTUs.

DATA AVAILABILITY STATEMENT

The datasets presented in this study can be found in online repositories. The names of the repository/repositories and accession number(s) can be found below: NCBI [accession: OM421748, OM501125, OM501126, OM468468, and PRJNA801354].

AUTHOR CONTRIBUTIONS

LB performed the microscopy observation, PCR experiment, data processing, and drafted the manuscript. LB, SZ, and XZ conducted the FISH and phylogenetic analysis. QZ and DJ designed the study and revised the manuscript. All authors contributed to the article and approved the submitted version.

FUNDING

This work was supported by the National Natural Science Foundation of China (project numbers: 31672251, 31772413, and 42176163), the Youth Innovation Promotion Association, CAS (No. 2019216), the Strategic Priority Research Program of the Chinese Academy of Sciences (No. XDA23050303), and the Key Research Program of Frontier Science, CAS (No. QYZDB-SSW-DQC013-1).

SUPPLEMENTARY MATERIAL

The Supplementary Material for this article can be found online at: https://www.frontiersin.org/articles/10.3389/fmars.2022.879388/full#supplementary-material

REFERENCES

Beinart, R. A., Rotterová, J., Čepička, I., Gast, R. J., and Edgcomb, V. P. (2018). The Genome of an Endosymbiotic Methanogen is Very Similar to Those of its Free-Living Relatives. *Environ. Microbiol.* 20 (7), 2538–2551. doi: 10.1111/1462-2920.14279

Boscaro, V., Husnik, F., Vannini, C., and Keeling, P. J. (2019). Symbionts of the Ciliate *Euplotes*: Diversity, Patterns and Potential as Models for Bacteria–Eukaryote Endosymbioses. *Proc. R. Soc. B: Biol. Sci.* 286 (1907), 20190693. doi: 10.1098/rspb.2019.0693

Bright, M., Espada-Hinojosa, S., Lagkouvardos, I., and Volland, J. M. (2014). The Giant Ciliate *Zoothamnium Niveum* and its Thiotrophic Epibiont *Candidatus* Thiobios Zoothamnicoli: A Model System to Study Interspecies Cooperation. *Front. Microbiol.* 5. doi: 10.3389/fmicb.2014.00145

Cai, L.-Z., Hwang, J.-S., Dahms, H.-U., Fu, S.-J., Chen, X.-W., and Wu, C. (2013). Does High Organic Matter Content Affect Polychaete Assemblages in a Shenzhen Bay Mudflat, China? *J. Marine Sci. Technol.* 21 (7), 37. doi: 10.6119/jmst-013-1223-5

Caporaso, J. G., Kuczynski, J., Stombaugh, J., Bittinger, K., Bushman, F. D., Costello, E. K., et al. (2010). QIIME Allows Analysis of High-Throughput Community Sequencing Data. *Nat. Methods* 7 (5), 335–336. doi: 10.1038/nmeth.f.303

Choi, K.-H., Kim, Y.-O., Lee, J.-B., Wang, S.-Y., Lee, M.-W., Lee, P.-G., et al. (2012). Thermal Impacts of a Coal Power Plant on the Plankton in an Open Coastal Water Environment. *J. Marine Sci. Technol.* 20 (2), 9. doi: 10.51400/2709-6998.1837

Dubilier, N., Bergin, C., and Lott, C. (2008). Symbiotic Diversity in Marine Animals: The Art of Harnessing Chemosynthesis. *Nat. Rev. Microbiol.* 6 (10), 725–740. doi: 10.1038/nrmicro1992

Edgcomb, V., Leadbetter, E., Bourland, W., Beaudoin, D., and Bernhard, J. (2011). Structured Multiple Endosymbiosis of Bacteria and Archaea in a Ciliate From Marine Sulfidic Sediments: A Survival Mechanism in Low Oxygen, Sulfidic Sediments? *Front. Microbiol.* 2. doi: 10.3389/fmicb.2011.00055

Embley, T. M., Finlay, B. J., and Brown, S. (1992). RNA Sequence Analysis Shows That the Symbionts in the Ciliate *Metopus* Contortus are Polymorphs of a Single Methanogen Species. *FEMS Microbiol. Lett.* 97 (1-2), 57–61. doi: 10.1111/j.1574-6968.1992.tb05439.x

Fenchel, T. (1969). The Ecology of Marine Microbenthos IV. Structure and Function of the Benthic Ecosystem, its Chemical and Physical Factors and the Microfauna Commuities With Special Reference to the Ciliated Protozoa. *Ophelia* 6 (1), 1–182. doi: 10.1080/00785326.1969.10409647

Fenchel, T., and Finlay, B. J. (1989). *Kentrophoros*: A Mouthless Ciliate With a Symbiotic Kitchen Garden. *Ophelia* 30 (2), 75–93.

Foissner, W. (1995). *Kentrophoros* (Ciliophora, Karyorelictea) has Oral Vestiges: A Reinvestigation of *K. Fistulosus* (FaurÉ-Fremiet 1950) Using Protargol Impregnation. *Archiv Für Protistenkunde* 146 (2), 165–179. doi: 10.1016/S0003-9365(11)80107-7

Fu, Y., Zheng, P., Zhang, X., Zhang, Q., and Ji, D. (2020). Protist Interactions and Seasonal Dynamics in the Coast of Yantai, Northern Yellow Sea of China as Revealed by Metabarcoding. *J. Ocean Univ. China* 19 (4), 961–974. doi: 10.1007/s11802-020-4461-x

Galtier, N., Gouy, M., and Gautier, C. (1996). SEAVIEW and PHYLO_WIN: Two Graphic Tools for Sequence Alignment and Molecular Phylogeny. *Bioinformatics* 12 (6), 543–548. doi: 10.1093/bioinformatics/12.6.543

Gao, S., Strüder-Kypke, M. C., Al-Rasheid, K. A. S., Lin, X., and Song, W. (2010). Molecular Phylogeny of Three Ambiguous Ciliate Genera: *Kentrophoros*, *Trachelolophos* and *Trachelotractus* (Alveolata, Ciliophora). *Zool Scripta* 39 (3), 305–313. doi: 10.1111/j.1463-6409.2010.00416.x

Gong, J., Qing, Y., Guo, X., and Warren, A. (2014). *Candidatus* Sonnebornia Yantaiensis a Member of Candidate Division OD1, as Intracellular Bacteria of the Ciliated Protist *Paramecium Bursaria* (Ciliophora, Oligohymenophorea). *Systematic Appl. Microbiol.* 37 (1), 35–41. doi: 10.1016/j.syapm.2013.08.007

Gong, J., Qing, Y., Zou, S., Fu, R., Su, L., Zhang, X., et al. (2016). Protist-Bacteria Associations: *Gammaproteobacteria* and *Alphaproteobacteria* Are Prevalent as Digestion-Resistant Bacteria in Ciliated Protozoa. *Front. Microbiol.* 7. doi: 10.3389/fmicb.2016.00498

Graf, J. S., Schorn, S., Kitzinger, K., Ahmerkamp, S., Woehle, C., Huettel, B., et al. (2021). Anaerobic Endosymbiont Generates Energy for Ciliate Host by Denitrification. *Nature* 591 (7850), 445–450. doi: 10.1038/s41586-021-03297-6

Hall, T., Biosciences, I., and Carlsbad, C. (2011). BioEdit: An Important Software for Molecular Biology. *GERF Bull. Biosci.* 2 (1), 60–61.

Lagkouvardos, I., Lesker, T. R., Hitch, T. C. A., Gálvez, E. J. C., Smit, N., Neuhaus, K., et al. (2019). Sequence and Cultivation Study of *Muribaculaceae* Reveals Novel Species, Host Preference, and Functional Potential of This Yet Undescribed Family. *Microbiome* 7 (1), 28. doi: 10.1186/s40168-019-0637-2

Lagkouvardos, I., Pukall, R., Abt, B., Foesel, B. U., Meier-Kolthoff, J. P., Kumar, N., et al. (2016). The Mouse Intestinal Bacterial Collection (miBC) Provides Host-Specific Insight Into Cultured Diversity and Functional Potential of the Gut Microbiota. *Nat. Microbiol.* 1 (10), 16131. doi: 10.1038/nmicrobiol.2016.131

Lanzoni, O., Plotnikov, A., Khlopko, Y., Munz, G., Petroni, G., and Potekhin, A. (2019). The Core Microbiome of Sessile Ciliate Stentor Coeruleus is Not Shaped by the Environment. *Sci. Rep.* 9 (1), 11356. doi: 10.1038/s41598-019-47701-8

Lei, Y., and Xu, K. (2008). Research Progress in the Ecology of Benthic Ciliated Protozoa. *Acta Hydrobiol Sin.* 32, 155–160. doi: 10.3724/sp.j.0000.2008.70155

Lind, A. E., Lewis, W. H., Spang, A., Guy, L., Embley, T. M., and Ettema, T. J. G. (2018). Genomes of Two Archaeal Endosymbionts Show Convergent Adaptations to an Intracellular Lifestyle. *ISME J.* 12 (11), 2655–2667. doi: 10.1038/s41396-018-0207-9

Martin, M. (2011). Cutadapt Removes Adapter Sequences From High-Throughput Sequencing Reads. *EMBnet J.* 17 (1), 10–12. doi: 10.14806/ej.17.1.200

Martinez-Garcia, M., Brazel, D., Poulton, N. J., Swan, B. K., Gomez, M. L., Masland, D., et al. (2012). Unveiling *in Situ* Interactions Between Marine Protists and Bacteria Through Single Cell Sequencing. *ISME J.* 6 (3), 703–707. doi: 10.1038/ismej.2011.126

Miyake, S., Ding, Y., Soh, M., Low, A., and Seedorf, H. (2020). Cultivation and Description of *Duncaniella Dubosii* Sp. Nov., *Duncaniella Freteri* Sp. Nov. And Emended Description of the Species *Duncaniella Muris*. *Int. J. Syst. Evol. Microbiol.* 70 (5), 3105–3110. doi: 10.1099/ijsem.0.004137

Muñoz-Gómez, S. A., Kreutz, M., and Hess, S. (2021). A Microbial Eukaryote With a Unique Combination of Purple Bacteria and Green Algae as Endosymbionts. *Sci. Adv.* 7 (24), eabg4102. doi: 10.1126/sciadv.abg4102

Nowack, E. C., and Melkonian, M. (2010). Endosymbiotic Associations Within Protists. Philosophical Transactions of the Royal Society of London. *Ser. B: Biol. Sci.* 365 (1541), 699–712. doi: 10.1098/rstb.2009.0188

Omar, A., Zhang, Q., Zou, S., and Gong, J. (2017). Morphology and Phylogeny of the Soil Ciliate *Metopus* Yantaiensis N. Sp. (Ciliophora, Metopida), With Identification of the Intracellular Bacteria. *J. Eukaryotic Microbiol.* 64 (6), 792–805. doi: 10.1111/jeu.12411

Ormerod, K. L., Wood, D. L. A., Lachner, N., Gellatly, S. L., Daly, J. N., Parsons, J. D., et al. (2016). Genomic Characterization of the Uncultured Bacteroidales Family S24-7 Inhabiting the Guts of Homeothermic Animals. *Microbiome* 4 (1), 36. doi: 10.1186/s40168-016-0181-2

Park, T., and Yu, Z. (2018). Do Ruminal Ciliates Select Their Preys and Prokaryotic Symbionts? *Front. Microbiol.* 9. doi: 10.3389/fmicb.2018.01710

Peng, Z. H., Jiao, S., and Wei, G. H. (2021). Research Methods of Microbial Biogeography. *Bio-protocol*, e2003930. doi: 10.21769/BioProtoc.2003930

Plotnikov, A. O., Balkin, A. S., Gogoleva, N. E., Lanzoni, O., Khlopko, Y. A., Cherkasov, S. V., et al. (2019). High-Throughput Sequencing of the 16S rRNA Gene as a Survey to Analyze the Microbiomes of Free-Living Ciliates Paramecium. *Microbial Ecol.* 78 (2), 286–298. doi: 10.1007/s00248-019-01321-x

Posada, D. (2008). Jmodeltest: Phylogenetic Model Averaging. *Mol. Biol. Evol.* 25 (7), 1253–1256. doi: 10.1093/molbev/msn083

Pruesse, E., Peplies, J., and Glöckner, F. O. (2012). SINA: Accurate High-Throughput Multiple Sequence Alignment of Ribosomal RNA Genes. *Bioinformatics* 28 (14), 1823–1829. doi: 10.1093/bioinformatics/bts252

Quast, C., Pruesse, E., Yilmaz, P., Gerken, J., Schweer, T., Yarza, P., et al. (2012). The SILVA Ribosomal RNA Gene Database Project: Improved Data Processing and Web-Based Tools. *Nucleic Acids Res.* 41 (1), 590–596. doi: 10.1093/nar/gks1219

Raikov, I. B. (1971). Bactéries Épizoiques Et Mode De Nutrition Du Cilié Psammophile *Kentrophoros Fistulosum* Fauré-Fremiet (Étude Au Microscope Électronique). *Protistologica* 7 (3), 365–378.

Ronquist, F., and Huelsenbeck, J. P. (2003). MrBayes 3: Bayesian Phylogenetic Inference Under Mixed Models. *Bioinformatics* 19 (12), 1572–1574. doi: 10.1093/bioinformatics/btg180

Rosati, G. (2002). "Ectosymbiosis in Ciliated Protozoa," in *Symbiosis: Mechanisms and Model Systems*. Ed. J. Seckbach (Dordrecht: Springer Netherlands), 475–488.

Salzman, N. H., de Jong, H., Paterson, Y., Harmsen, H. J. M., Welling, G. W., and Bos, N. A. (2002). Analysis of 16S Libraries of Mouse Gastrointestinal Microflora Reveals a Large New Group of Mouse Intestinal Bacteria. *Microbiology* 148 (11), 3651–3660. doi: 10.1099/00221287-148-11-3651

Schloss, P. D., Westcott, S. L., Ryabin, T., Hall, J. R., Hartmann, M., Hollister, E. B., et al. (2009). Introducing Mothur: Open-Source, Platform-Independent, Community-Supported Software for Describing and Comparing Microbial Communities. *Appl. Environ. Microbiol.* 75 (23), 7537–7541. doi: 10.1128/AEM.01541-09

Scholz, C. F. P., and Kilian, M. (2016). The Natural History of Cutaneous Propionibacteria, and Reclassification of Selected Species Within the Genus *Propionibacterium* to the Proposed Novel Genera *Acidipropionibacterium* Gen. Nov., *Cutibacterium* Gen. Nov. And *Pseudopropionibacterium* Gen. Nov. *Int. J. Systematic Evol Microbiol.* 66 (11), 4422–4432. doi: 10.1099/ijsem.0.001367

Seah, B. K. B., Antony, C. P., Huettel, B., Zarzycki, J., Schada von Borzyskowski, L., Erb, T. J., et al. (2019). Sulfur-Oxidizing Symbionts Without Canonical Genes for Autotrophic CO_2 Fixation. *mBio* 10 (3), e01112–e01119. doi: 10.1128/mBio.01112-19

Seah, B. K. B., Schwaha, T., Volland, J.-M., Huettel, B., Dubilier, N., and Gruber-Vodicka, H. R. (2017). Specificity in Diversity: Single Origin of a Widespread Ciliate-Bacteria Symbiosis. *Proc. R. Soc. B: Biol. Sci.* 284 (1858), 20170764. doi: 10.1098/rspb.2017.0764

Stamatakis, A. (2014). RAxML Version 8: A Tool for Phylogenetic Analysis and Post-Analysis of Large Phylogenies. *Bioinformatics* 30 (9), 1312–1313. doi: 10.1093/bioinformatics/btu033

Tamura, K., Stecher, G., Peterson, D., Filipski, A., and Kumar, S. (2013). MEGA6: Molecular Evolutionary Genetics Analysis Version 6.0. *Mol. Biol. Evol.* 30 (12), 2725–2729. doi: 10.1093/molbev/mst197

Van Valkenburgh, B. (1991). Iterative Evolution of Hypercarnivory in Canids (Mammalia: Carnivora): Evolutionary Interactions Among Sympatric Predators. *Paleobiology* 17 (4), 340–362. doi: 10.1017/S0094837300010691

Volland, J.-M., Schintlmeister, A., Zambalos, H., Reipert, S., Mozetič, P., Espada-Hinojosa, S., et al (2018). NanoSIMS and Tissue Autoradiography Reveal Symbiont Carbon Fixation and Organic Carbon Transfer To Giant Ciliate Host. *ISME J.* 12(3), 714–727. doi: 10.1038/s41396-018-0069-1

Wang, Y., Ji, D., and Yin, J. (2019). Morphology and Phylogeny of Two *Phialina* Species (Ciliophora, Haptoria) From Northern China. *Eur. J. Protistol* 67, 46–58. doi: 10.1016/j.ejop.2018.10.002

Wilbert, N., and Song, W. (2005). New Contributions to the Marine Benthic Ciliates From the Antarctic Area, Including Description of Seven New Species (Protozoa, Ciliophora). *J. Natural History* 39 (13), 935–973. doi: 10.1080/00222930400001509

Xu, Y., Huang, J., Warren, A., Al-Rasheid, K. A. S., Al-Farraj, S. A., and Song, W. (2011). Morphological and Molecular Information of a New Species of *Geleia* (Ciliophora, Karyorelictea), With Redescriptions of Two *Kentrophoros* Species From China. *Eur. J. Protistol* 47 (3), 172–185. doi: 10.1016/j.ejop.2011.03.003

Yılmaz, L.Ş., and Noguera, D. R. (2007). Development of Thermodynamic Models for Simulating Probe Dissociation Profiles in Fluorescence *in Situ* Hybridization. *Biotechnol. Bioengineering* 96 (2), 349–363. doi: 10.1002/bit.21114

Zhou, W., Qi, D., Swaisgood, R. R., Wang, L., Jin, Y., Wu, Q., et al. (2021). Symbiotic Bacteria Mediate Volatile Chemical Signal Synthesis in a Large Solitary Mammal Species. *ISME J.* 15 (7), 2070–2080. doi: 10.1038/s41396-021-00905-1

Conflict of Interest: The authors declare that the research was conducted in the absence of any commercial or financial relationships that could be construed as a potential conflict of interest.

Publisher's Note: All claims expressed in this article are solely those of the authors and do not necessarily represent those of their affiliated organizations, or those of the publisher, the editors and the reviewers. Any product that may be evaluated in this article, or claim that may be made by its manufacturer, is not guaranteed or endorsed by the publisher.